


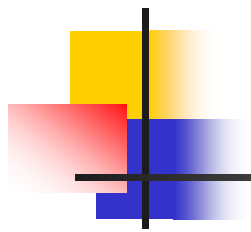
Precision tests of electromagnetism and relativistic gravity



Wei-Tou Ni

*Center for Gravitation and Cosmology (CGC),
Department of Physics, National Tsing Hua U.*

A chapter for the book "Electromagnetism" (ISBN 979-953-307-400-8) by INTECH (open access), to be published February, 2012 [[arXiv:1109.5501](https://arxiv.org/abs/1109.5501)]



1	Chapter Number
2	Foundations of Electromagnetism, Equivalence
3	Principles and Cosmic Interactions
4	Wei-Tou Ni
5	<i>Center for Gravitation and Cosmology</i>
6	<i>Department of Physics, National Tsing Hua University</i>
7	<i>Hsinchu, Taiwan, ROC,</i>
8	<i>Shanghai United Center for Astrophysics</i>
9	<i>Shanghai Normal University, Shanghai,</i>
10	<i>China</i>
11	1. Introduction
12	Standard electromagnetism is based on Maxwell equations and Lorentz force law. It can be
13	derived by a least action with the following Lagrangian density for a system of charged
14	particles in Gaussian units (e.g., Jackson, 1999),
15	$L_{EMS}=L_{EM}+L_{EM-P}+L_P=-\frac{1}{(16\pi)}\left[\frac{1}{2}\eta^{ik}\eta^{jl}-\frac{1}{2}\eta^{il}\eta^{kj}\right]F_{ij}F_{kl}-A_{kj}^k-\sum_I m_I\left[\frac{ds_I}{dt}\right]\delta(\mathbf{x}-\mathbf{x}_I), \quad (1)$
2012.03.04.	APs
2012	Precision of EM and relativistic gravity
	WTNi



Outline

- Introduction & Photon mass constraints
- Quantum corrections – quantum corrections
- Parametrized Post-Maxwell (PPM) electrodynamics
- Electromagnetic wave propagation in PPM
- Measuring the parameters of the PPM electrodynamics
- Electrodynamics in curved spacetime and EEP
- Empirical tests of electromagnetism and the χ -g framework
- Pseudoscalar-photon interaction and the cosmic pol. rotation
- Solar-system tests of DSSY inflation model with a Weyl term
- Discussion on DGP and massive GR and outlook

An example
of Accuracy

Measurement of Light Velocity in History

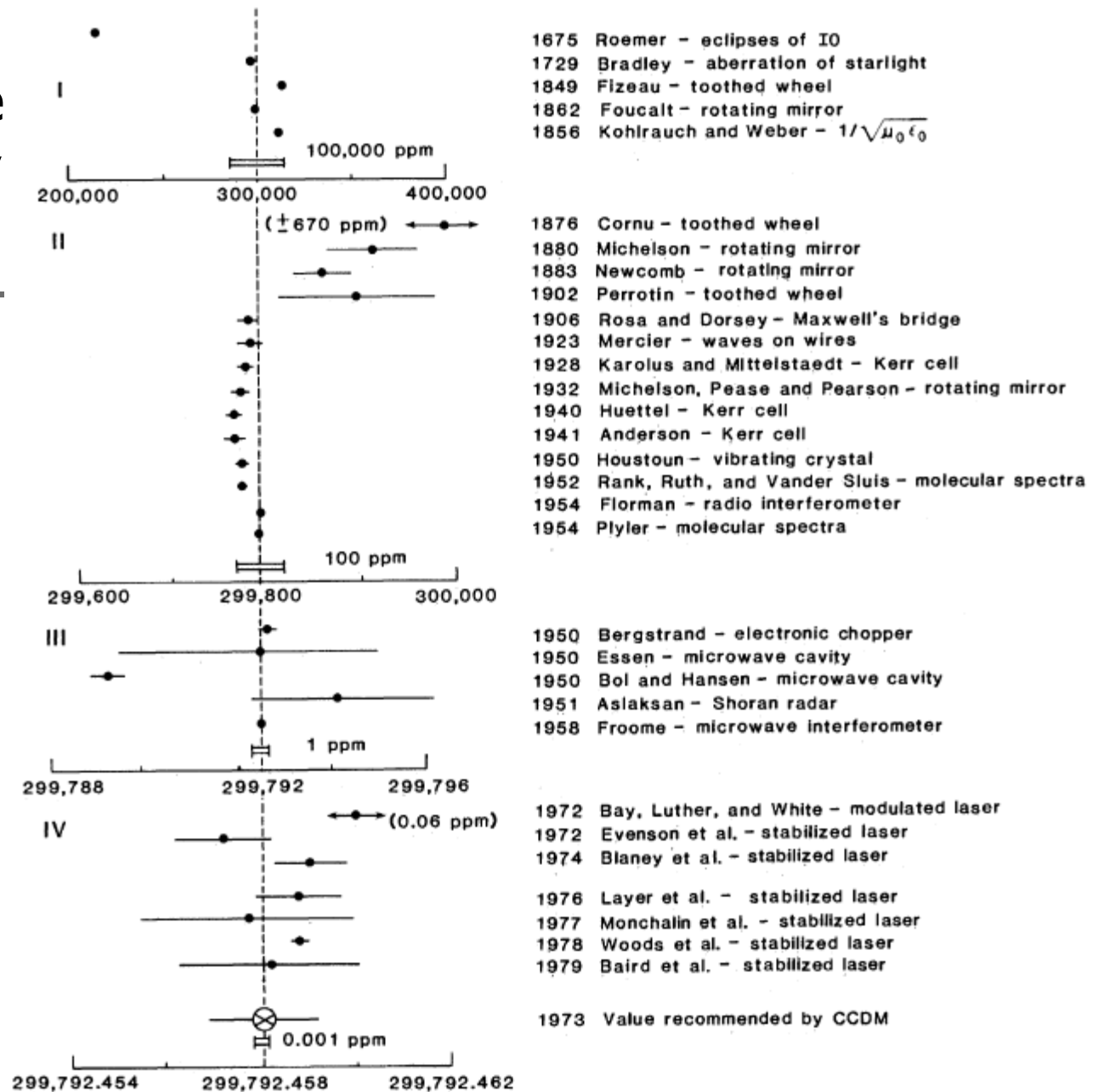


Fig. 3. Graph showing the measured values of the speed of light. The graph is divided into four regions and the horizontal scale is different in each region; the vertical line corresponds to the same value in each region.

List of experiments measuring the limiting velocity of neutrinos

Experiment	Baseline	Average Energy	Relative Measurement	$ (v-c) /c$
Alspector et al. (1976)	0.55 km		$\leq 4 \times 10^{-4}$ (99% confidence level)	
Kalbfleisch (1979).	0.55 km		$\leq 4 \times 10^{-5}$ (95% confidence level)	
SN1987a				2×10^{-9}
MINOS (2006)	734 km			$(v-c)/c = (5.1 \pm 2.9) \times 10^{-5}$
OPERA (2011)	730 km	17 GeV		$(v-c)/c = (2.48 \pm 0.28$ (stat.) ± 0.30 (sys)) $\times 10^{-5}$

The OPERA result is retracted. (GPS problem [loose fibre connection])



Ans.:No direct distance could be measured through Earth's crust
except neutrino experiments.

Can Fundamental Physics Experiments Contribute to Geodesy?

Lagrangian density L_{EMS} for a system of charged particles in Gaussian units

- $L_{EMS} = L_{EM} + L_{EM-P} + L_P$
$$= -(1/(16\pi))[(1/2)\eta^{ik}\eta^{jl} - (1/2)\eta^{il}\eta^{kj}]F_{ij}F_{kl}$$

$$- A_k j^k - \sum_I m_I [(ds_I)/(dt)]\delta(\mathbf{x} - \mathbf{x}_I),$$
- L_{EMS} Lagrangian density for EM system
- L_{EM} Lagrangian density for EM field
- L_{EM-P} *Lagrangian density for EM field-Particle interaction*
- L_P Particle Lagrangian

Proca (1936-8) Lagrangian density and mass of photon soon after Yukawa interaction was proposed

- $L_{Proca} = (m_{photon}^2 c^2 / 8\pi\hbar^2)(A_k A^k)$
- the Coulomb law is modified to have the electric potential $A_0 = q(e^{-\mu r} / r)$
- where q is the charge of the source particle, r is the distance to the source particle, and μ ($\equiv m_{photon} c / \hbar$) gives the inverse range of the interaction

Constraints on the mass of photon

Williams, Faller & Hill (1971) Lab Test	$m_{\text{photon}} \leq 10^{-14} \text{ eV}$ (= $2 \times 10^{-47} \text{ g}$)	$\mu^1 \geq 2 \times 10^7 \text{ m}$
Davis, Goldhaber & Nieto (1975) Pioneer 10 Jupiter flyby	$m_{\text{photon}} \leq 4 \times 10^{-16} \text{ eV}$ (= $7 \times 10^{-49} \text{ g}$)	$\mu^1 \geq 5 \times 10^8 \text{ m}$
Ryutov (2007) Solar wind magnetic field	$m_{\text{photon}} \leq 10^{-18} \text{ eV}$ (= $2 \times 10^{-51} \text{ g}$)	$\mu^1 \geq 2 \times 10^{11} \text{ m}$
Chibisov (1976) galactic sized fields	$m_{\text{photon}} \leq 2 \times 10^{-27} \text{ eV}$ (= $4 \times 10^{-60} \text{ g}$)	$\mu^1 \geq 10^{20} \text{ m}$

If cosmic scale magnetic field is discovered, the constraint on the interaction range may become bigger or comparable to Hubble distance (of the order of radius of curvature of our observable universe). If this happens, the concept of photon mass may lose significance to cosmology amid gravity coupling or curvature coupling of photons.

Quantum corrections to classical electrodynamics

Heisenberg-Euler Lagrangian

$$L_{\text{Heisenberg-Euler}} = [2\alpha^2\hbar^2/45(4\pi)^2m^4c^6][(\mathbf{E}^2-\mathbf{B}^2)^2 + 7(\mathbf{E}\cdot\mathbf{B})^2], \quad (10)$$

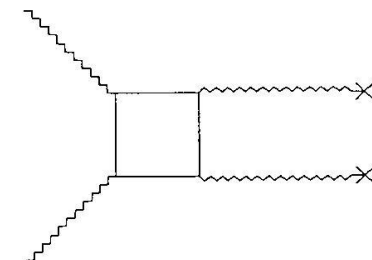
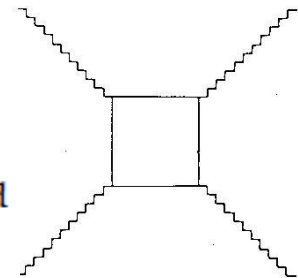
where α is the fine structure constant and m the electron mass. In terms of critical field strength B_c defined as

$$B_c \equiv E_c \equiv m^2c^3/e\hbar = 4.4 \times 10^{13} \text{ G} = 4.4 \times 10^9 \text{ T} = 4.4 \times 10^{13} \text{ statvolt/cm} = 1.3 \times 10^{18} \text{ V/m}, \quad (11)$$

this Lagrangian density can be written as

$$L_{\text{Heisenberg-Euler}} = (1/8\pi) B_c^{-2} [\eta_1(\mathbf{E}^2-\mathbf{B}^2)^2 + 4\eta_2(\mathbf{E}\cdot\mathbf{B})^2], \quad (12)$$

$$\eta_1 = \alpha/(45\pi) = 5.1 \times 10^{-5} \text{ and } \eta_2 = 7\alpha/(180\pi) = 9.0 \times 10^{-5}. \quad (13)$$



For time varying and space varying external fields, and higher order corrections in quantum electrodynamics, please see Dittrich and Reuter (1985) and Kim (2011) and references therein.



Born-Infeld Electrodynamics

Before Heisenberg & Euler (1936), Born and Infeld (Born, 1934; Born & Infeld, 1934) proposed the following Lagrangian density for the electromagnetic field

$$L_{\text{Born-Infeld}} = -(b^2/4\pi) [1 - (\mathbf{E}^2 - \mathbf{B}^2)/b^2 - (\mathbf{E} \cdot \mathbf{B})^2/b^4]^{1/2}, \quad (14)$$

where b is a constant which gives the maximum electric field strength. For field strength small compared with b , (14) can be expanded into

$$L_{\text{Born-Infeld}} = (1/8\pi) [(\mathbf{E}^2 - \mathbf{B}^2) + (\mathbf{E}^2 - \mathbf{B}^2)^2/b^2 + (\mathbf{E} \cdot \mathbf{B})^2/b^2 + \mathcal{O}(b^{-4})]. \quad (15)$$

The lowest order of Born-Infeld electrodynamics agrees with the classical electrodynamics. The next order corrections are of the form of Eq. (12) with

$$\eta_1 = \eta_2 = B_c^2/b^2. \quad (16)$$

In the Born-Infeld electrodynamics, b is the maximum electric field. Electric fields at the edge of heavy nuclei are of the order of 10^{21} V/m. If we take b to be 10^{21} V/m, then, $\eta_1 = \eta_2 = 5.9 \times 10^{-6}$.

Parametrized Post-Maxwell (PPM)

Lagrangian density

(4 parameters: $\xi, \eta_1, \eta_2, \eta_3$)

- $L_{PPM} = (1/8\pi) \{ (\mathbf{E}^2 - \mathbf{B}^2) + \xi \Phi(\mathbf{E} \cdot \mathbf{B}) + B_c^{-2} [\eta_1 (\mathbf{E}^2 - \mathbf{B}^2)^2 + 4\eta_2 (\mathbf{E} \cdot \mathbf{B})^2 + 2\eta_3 (\mathbf{E}^2 - \mathbf{B}^2)(\mathbf{E} \cdot \mathbf{B})] \}$
- $L_{PPM} = (1/(32\pi)) \{ -2F^{kl}F_{kl} - \xi \Phi F^{*kl}F_{kl} + B_c^{-2} [\eta_1 (F^{kl}F_{kl})^2 + \eta_2 (F^{*kl}F_{kl})^2 + \eta_3 (F^{kl}F_{kl})(F^{*ij}F_{ij})] \}$
(manifestly Lorentz invariant form)
- Dual electromagnetic field $F^{*ij} \equiv (1/2)e^{ijkl} F_{kl}$

Unified theory of nonlinear electrodynamics and gravity

A. Torres-Gomez, K. Krasnov, & C. Scarinci PRD 83, 025023 (2011)

- A class of unified theories of electromagnetism and gravity with Lagrangian of the BF type (F: Curvature of the connection 1-form A (ω), with a potential for the B (Σ) field (Lie-algebra valued 2-form), the gauge group is U(2) (complexified).
- Given a choice of the potential function the theory is a deformation of (complex) general relativity and electromagnetism.

if we want to think of A^4 as the $u(1)$ component of a connection field, gives the correct Lorentzian signature action. Thus, for

$$A^4 = i\mathbf{A}, \quad \mathbf{A} \in \mathbb{R}, \quad (36)$$

we get

$$S[\mathbf{A}] = -\frac{1}{4g_{u(1)}^2} \int d^4x F^{\mu\nu} F_{\mu\nu}, \quad (37)$$

$$(\epsilon^{\mu\nu\rho\sigma} F_{\mu\nu}^4 F_{\rho\sigma}^4)^2 = -8(F^{4\mu\nu} F_{\mu\nu}^4)^2 + 16F_{\mu}^{4\nu} F_{\nu}^{4\rho} F_{\rho}^{4\sigma} F_{\sigma}^{4\mu}, \quad (44)$$

we get the following Lagrangian:

$$\begin{aligned} \mathcal{L}^{(4)} = & \frac{1}{16} (F^{4\mu\nu} F_{\mu\nu}^4)^2 \left(\frac{3\chi}{(\alpha + \gamma)^4} - \frac{2\delta}{\gamma^2(\alpha + \gamma)^2} + \frac{3\xi}{\gamma^4} \right) \\ & - \frac{1}{4} F_{\mu}^{4\nu} F_{\nu}^{4\rho} F_{\rho}^{4\sigma} F_{\sigma}^{4\mu} \left(\frac{\chi}{(\alpha + \gamma)^4} - \frac{2\delta}{\gamma^2(\alpha + \gamma)^2} + \frac{\xi}{\gamma^4} \right) \\ & - \frac{i}{4} (F^{4\mu\nu} F_{\mu\nu}^4) (\epsilon^{\alpha\beta\gamma\delta} F_{\alpha\beta}^4 F_{\gamma\delta}^4) \left(\frac{\chi}{(\alpha + \gamma)^4} - \frac{\xi}{\gamma^4} \right). \end{aligned}$$

Generalized Uncertainty Principle, Blackhole Entropy and modified Newton's law

(Pisin's talk & Bernard Carr's talk in LeCosPA)

- When applying it to the entropic interpretation, we demonstrate that the resulting gravity force law does include **sub-leading order correction terms that depend on h-bar**.
- Such deviation from the classical Newton's law may serve as a probe to the validity of the entropic gravity postulate.
- Modified force law

$$F_{\text{GUP}} = F_N \left\{ 1 + \alpha [2 - \text{Log}\alpha] + \alpha^2 [4 - 5\text{Log}\alpha + (\text{Log}\alpha)^2] + \alpha^3 [7 - 18\text{Log}\alpha + 8(\text{Log}\alpha)^2 - (\text{Log}\alpha)^3] + \dots \right\} .$$

Here $F_N = GmM/R^2$ is Newton's gravitational force law, and we have introduced symbols $\eta = \sqrt{1 - 4G\hbar/c^3 R^2}$ and $\alpha = G\hbar/c^3 R^2$ to simplify the expression.

Equations for nonlinear electrodynamics (1)

In analogue with the nonlinear electrodynamics of continuous media, we can define the electric displacement \mathbf{D} and magnetic field \mathbf{H} as follows:

$$\mathbf{D} \equiv 4\pi(\partial L_{PPM}/\partial \mathbf{E}) = [1 + 2\eta_1(\mathbf{E}^2 - \mathbf{B}^2)B_c^{-2} + 2\eta_3(\mathbf{E} \cdot \mathbf{B})B_c^{-2}] \mathbf{E} + [\Phi + 4\eta_2(\mathbf{E} \cdot \mathbf{B})B_c^{-2} + \eta_3(\mathbf{E}^2 - \mathbf{B}^2)B_c^{-2}] \mathbf{B}, \quad (21)$$

$$\mathbf{H} \equiv -4\pi(\partial L_{PPM}/\partial \mathbf{B}) = [1 + 2\eta_1(\mathbf{E}^2 - \mathbf{B}^2)B_c^{-2} + 2\eta_3(\mathbf{E} \cdot \mathbf{B})B_c^{-2}] \mathbf{B} - [\Phi + 4\eta_2(\mathbf{E} \cdot \mathbf{B})B_c^{-2} + \eta_3(\mathbf{E}^2 - \mathbf{B}^2)B_c^{-2}] \mathbf{E}. \quad (22)$$

From \mathbf{D} & \mathbf{H} , we can define a second-rank G_{ij} tensor, just like from \mathbf{E} & \mathbf{B} to define F_{ij} tensor. With these definitions and following the standard procedure in electrodynamics [see, e.g., Jackson (1999), p. 599], the nonlinear equations of the electromagnetic field are

$$\text{curl } \mathbf{H} = (1/c) \partial \mathbf{D} / \partial t + 4\pi \mathbf{J}, \quad (23)$$

$$\text{div } \mathbf{D} = 4\pi \rho, \quad (24)$$

$$\text{curl } \mathbf{E} = -(1/c) \partial \mathbf{B} / \partial t, \quad (25)$$

$$\text{div } \mathbf{B} = 0. \quad (26)$$

Equations for nonlinear electrodynamics (2)

We notice that it has the same form as in macroscopic electrodynamics. The Lorentz force law remains the same as in classical electrodynamics:

$$d[(1-\mathbf{v}_I^2/c^2)^{-1/2}m_I\mathbf{v}_I]/dt = q_I[\mathbf{E} + (1/c)\mathbf{v}_I \times \mathbf{B}] \quad (27)$$

for the I -th particle with charge q_I and velocity \mathbf{v}_I in the system. The source of Φ in this system is $(\mathbf{E} \cdot \mathbf{B})$ and the field equation for Φ is

$$\partial^j L_\Phi / \partial(\partial^i \Phi) - \partial L_\Phi / \partial \Phi = \mathbf{E} \cdot \mathbf{B}, \quad (28)$$

where L_Φ is the Lagrangian density of the pseudoscalar field Φ .

Electromagnetic wave propagation in PPM electrodynamics

Here we follow the previous method (Ni et al., 1991; Ni, 1998), and separate the electric field and magnetic induction field into the wave part (small compared to external part) and external part as follows:

$$\mathbf{E} = \mathbf{E}^{\text{wave}} + \mathbf{E}^{\text{ext}}, \quad (29)$$

$$\mathbf{B} = \mathbf{B}^{\text{wave}} + \mathbf{B}^{\text{ext}}, \quad (30)$$

We use the following expressions to calculate the displacement field $\mathbf{D}^{\text{wave}} [= (D^{\text{wave}}_a) = (D^{\text{wave}}_1, D^{\text{wave}}_2, D^{\text{wave}}_3)]$ and the magnetic field $\mathbf{H}^{\text{wave}} [= (H^{\text{wave}}_a) = (H^{\text{wave}}_1, H^{\text{wave}}_2, H^{\text{wave}}_3)]$ of the electromagnetic waves:

$$D^{\text{wave}}_a = D_a - D^{\text{ext}}_a = (4\pi)[(\partial L_{\text{PPM}}/\partial E_a)_{\mathbf{E}\&\mathbf{B}} - (\partial L_{\text{PPM}}/\partial E_a)_{\text{ext}}], \quad (31)$$

$$H^{\text{wave}}_a = H_a - H^{\text{ext}}_a = - (4\pi)[(\partial L_{\text{PPM}}/\partial B_a)_{\mathbf{E}\&\mathbf{B}} - (\partial L_{\text{PPM}}/\partial B_a)_{\text{ext}}], \quad (32)$$

where (...) $_{\mathbf{E}\&\mathbf{B}}$ means that the quantity inside paranthesis is evaluated at the total field values \mathbf{E} & \mathbf{B} and (...) $_{\text{ext}}$ means that the quantity inside paranthesis is evaluated at the external field values \mathbf{E}^{ext} & \mathbf{B}^{ext} .

Since both the total field and the external field satisfy Eqs. (23)-(26), the wave part also satisfy the same form of Eqs. (23)-(26) with the source terms subtracted:

$$\text{curl } \mathbf{H}^{\text{wave}} = (1/c) \partial \mathbf{D}^{\text{wave}} / \partial t, \quad (33)$$

$$\text{div } \mathbf{D}^{\text{wave}} = 0, \quad (34)$$

$$\text{curl } \mathbf{E}^{\text{wave}} = -(1/c) \partial \mathbf{B}^{\text{wave}} / \partial t, \quad (35)$$

$$\text{div } \mathbf{B}^{\text{wave}} = 0. \quad (36)$$

After calculating D^{wave}_a and H^{wave}_a from Eqs. (31) & (32), we express them in the following form:

$$D^{\text{wave}}_a = \sum_{\beta=1}^3 \varepsilon_{\alpha\beta} E^{\text{wave}}_\beta + \sum_{\beta=1}^3 \lambda_{a\beta} B^{\text{wave}}_\beta, \quad (37)$$

$$H^{\text{wave}}_a = \sum_{\beta=1}^3 (\mu^{-1})_{\alpha\beta} B^{\text{wave}}_\beta - \sum_{\beta=1}^3 \lambda_{\beta a} E^{\text{wave}}_\beta, \quad (38)$$

where

$$\varepsilon_{\alpha\beta} = \delta_{\alpha\beta} [1 + 2\eta_1 (\mathbf{E}^2 - \mathbf{B}^2) B_c^{-2} + 2\eta_3 (\mathbf{E} \cdot \mathbf{B}) B_c^{-2}] + 4\eta_1 E_\alpha E_\beta B_c^{-2} + 4\eta_2 B_\alpha B_\beta B_c^{-2} + 2\eta_3 (E_\alpha B_\beta + E_\beta B_\alpha) B_c^{-2}, \quad (39)$$

Using eikonal approximation, we look for plane-wave solutions. Choose the z-axis in the propagation direction. Solving the dispersion relation for ω , we obtain

$$\omega_{\pm} = k \{1 + (1/4) [(J_1+J_2) \pm [(J_1-J_2)^2 + 4J^2]^{1/2}]\}, \quad (42)$$

where

$$J_1 \equiv (\mu^{-1})_{22} - \varepsilon_{11} - 2\lambda_{12}, \quad (43)$$

$$J_2 \equiv (\mu^{-1})_{11} - \varepsilon_{22} + 2\lambda_{21}, \quad (44)$$

$$J \equiv -\varepsilon_{12} - (\mu^{-1})_{12} + \lambda_{11} - \lambda_{22}. \quad (45)$$

Since the index of refraction n is

$$n = k/\omega, \quad (46)$$

we find

$$n_{\pm} = 1 - (1/4) \{(J_1+J_2) \pm [(J_1-J_2)^2 + 4J^2]^{1/2}\}. \quad (47)$$

From this formula, we notice that “no birefringence” is equivalent to $J_1=J_2$ and $J=0$. A sufficient condition for this to happen is $\eta_1 = \eta_2$, $\eta_3 = 0$, and no constraint on ξ . We will show in the following that this is also a necessary condition. The Born-Infeld electrodynamics satisfies this condition and has no birefringence in the theory.



Birefringence or no Birefringence

Using Eq. (47), we obtain the indices of refraction for this case:

$$n_{\pm} = 1 + \{(\eta_1 + \eta_2) \pm [(\eta_1 - \eta_2)^2 + \eta_3^2]^{1/2}\} (B_1^2 + B_2^2) B_c^{-2}. \quad (54)$$

The condition of no birefringence in Eq. (54) means that $[(\eta_1 - \eta_2)^2 + \eta_3^2]$ vanishes, i.e.,

$$\eta_1 = \eta_2, \quad \eta_3 = 0, \quad \text{and no constraint on } \xi \quad (55)$$

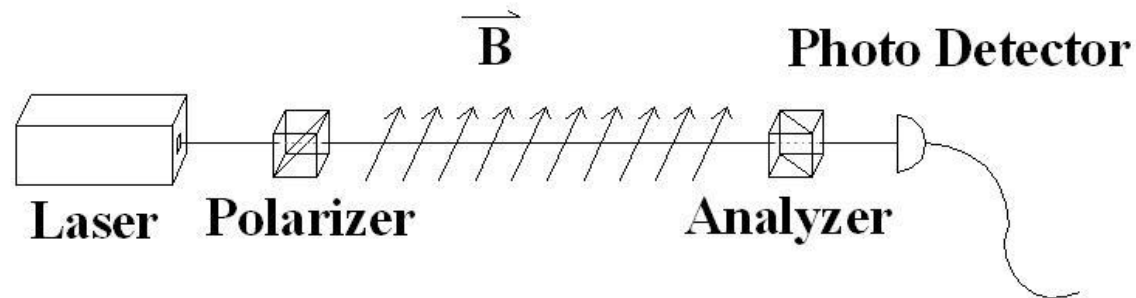
This shows that Eq. (55) is a necessary condition for no birefringence. For $\mathbf{E}^{\text{ext}} = 0$, the refractive indices in the transverse external magnetic field \mathbf{B}^{ext} for the linearly polarized lights whose polarizations are parallel and orthogonal to the magnetic field, are as follows:

$$n_{\parallel} = 1 + \{(\eta_1 + \eta_2) + [(\eta_1 - \eta_2)^2 + \eta_3^2]^{1/2}\} (\mathbf{B}^{\text{ext}})^2 B_c^{-2} \quad (\mathbf{E}^{\text{wave}} \parallel \mathbf{B}^{\text{ext}}), \quad (56)$$

$$n_{\perp} = 1 + \{(\eta_1 + \eta_2) - [(\eta_1 - \eta_2)^2 + \eta_3^2]^{1/2}\} (\mathbf{B}^{\text{ext}})^2 B_c^{-2} \quad (\mathbf{E}^{\text{wave}} \perp \mathbf{B}^{\text{ext}}). \quad (57)$$

Measuring the parameters of the PPM electrodynamics

- $\Delta n = n_{\parallel} - n_{\perp} = 4.0 \times 10^{-24} (\mathbf{B}^{\text{ext}}/1\text{T})^2$



Measuring the parameters of the PPM electrodynamics

- Let's choose z -axis to be in the propagation direction, x -axis in the \mathbf{E}^{ext} direction and y -axis in the \mathbf{B}^{ext} direction, i.e., $\mathbf{k} = (0, 0, k)$, $\mathbf{E}^{\text{ext}} = (E, 0, 0)$ and $\mathbf{B}^{\text{ext}} = (0, B, 0)$.

- $n_{\pm} = 1 + (\eta_1 + \eta_2)(E^2 + B^2 - EB)B_c^{-2} \pm [(\eta_1 - \eta_2)^2(E^2 + B^2 - EB)^2 + \eta_3^2(E^2 - B^2)]^{1/2} B_c^{-2}$.

- (i) $E=B$ as in the strong microwave cavity, the indices of refraction for light is

- $$n_{\pm} = 1 + (\eta_1 + \eta_2)B^2 B_c^{-2} \pm (\eta_1 - \eta_2)B^2 B_c^{-2},$$

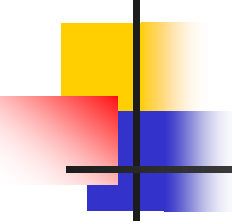
with birefringence Δn given by

$$\Delta n = 2(\eta_1 - \eta_2)B^2 B_c^{-2};$$

- (ii) $E=0, B \neq 0$, the indices of refraction for light is

$$n_{\pm} = 1 + (\eta_1 + \eta_2)B^2 B_c^{-2} \pm [(\eta_1 - \eta_2)^2 + \eta_3^2]^{1/2} B^2 B_c^{-2},$$

$$\Delta n = 2[(\eta_1 - \eta_2)^2 + \eta_3^2]^{1/2} B^2 B_c^{-2}.$$



Measuring the parameters of the PPM electrodynamics

To measure η_1 , η_2 and η_3 , we could do the following three experiments to determine them: (i) to measure the birefringence $\Delta n = 2(\eta_1 - \eta_2)B^2B_c^{-2}$ of light with the external field provided by a strong microwave cavity or wave guide to determine $\eta_1 - \eta_2$; (ii) to measure the birefringence $\Delta n = 2[(\eta_1 - \eta_2)^2 + \eta_3^2]^{1/2}B^2B_c^{-2}$ of light with the external magnetic field provided by a strong magnet to determine η_3 with $\eta_1 - \eta_2$ determined by (i); (iii) to measure η_1 and η_2 separately using two-arm interferometer with the paths in two arms in magnetic fields with different strengths (or one with no magnetic field).

As to the term $\xi\Phi$ and parameter ξ , it does not give any change in the index of refraction. However, as we will see in section 7 and section 8, it gives a polarization rotation and the effect can be measured through observations with astrophysical and cosmological propagation of electromagnetic waves.

Lab Experiment: Principle of Experiment

Vacuum Dichroism, Pseudoscalar-Photon Interaction and Millicharged Fermions

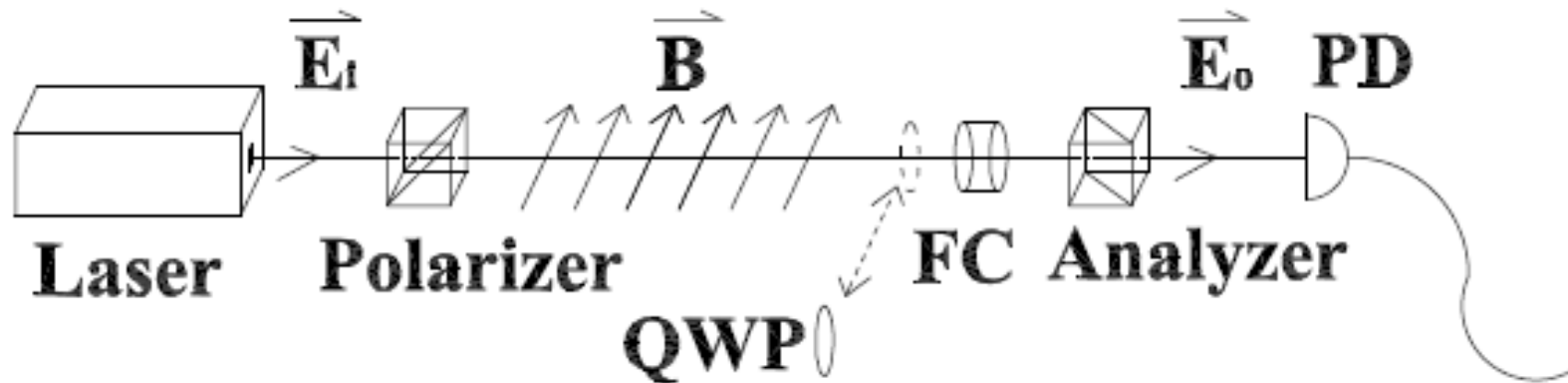


Fig. 1. Principle of vacuum dichroism and birefringence measurement.

Apparatus and Finesse Measurement

Vacuum Dichroism, Pseudoscalar-Photon Interaction and Millicharged Fermions 2821



Fig. 3. A picture of experimental apparatus.

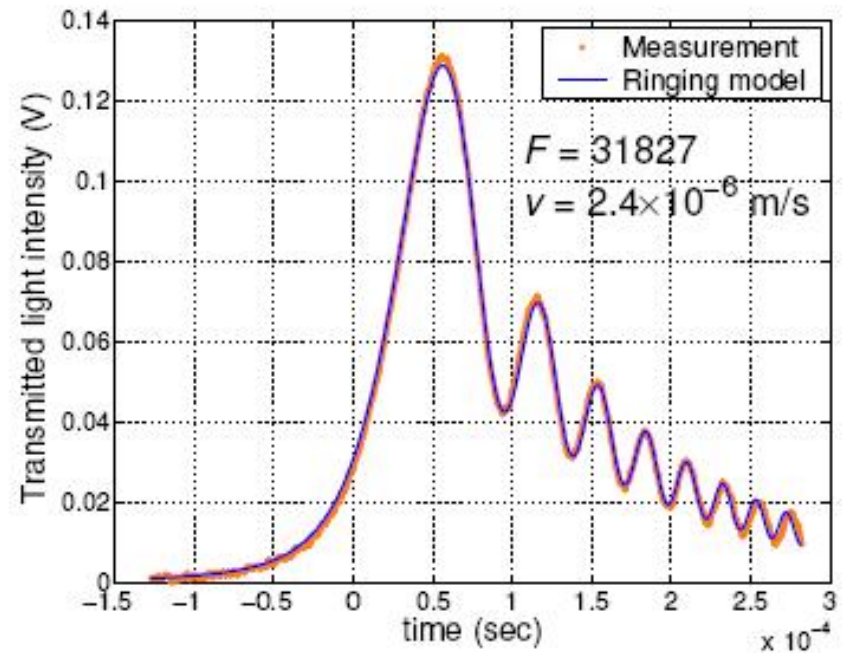


Fig. 4. A finesse measurement with fitting.

Suspension and Analyzer's Extinction ratio

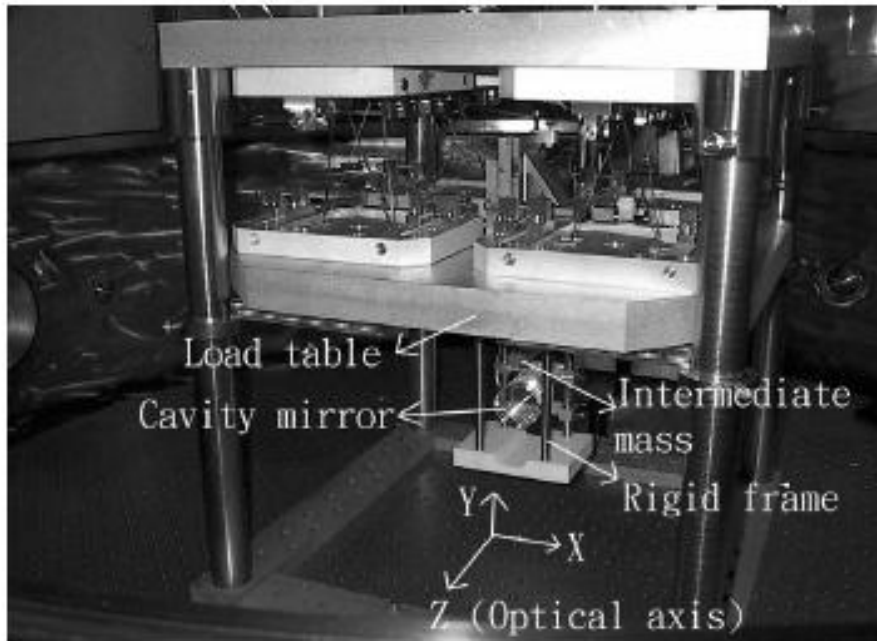


Fig. 5. Picture of one of our X-pendulum-double-pendulum suspension system.

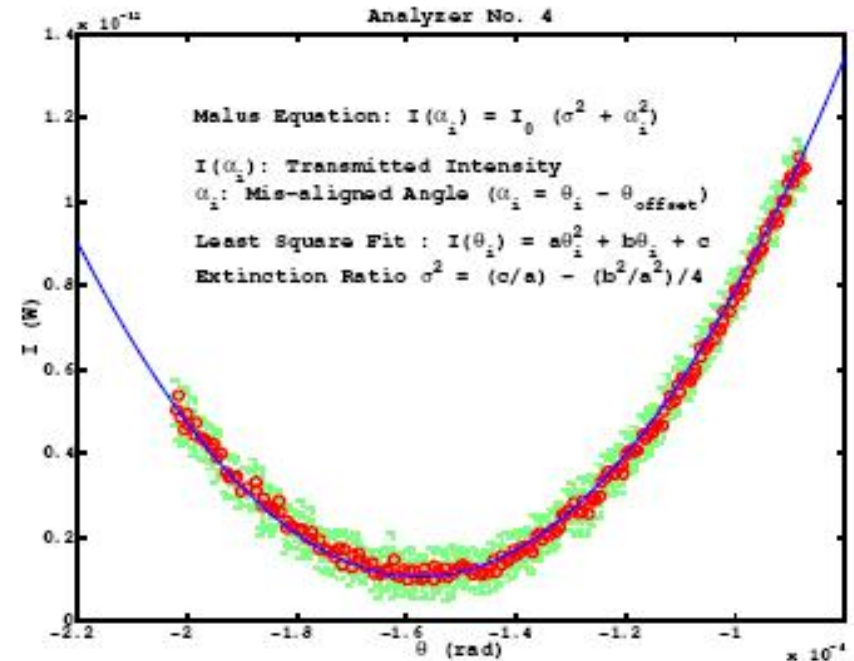
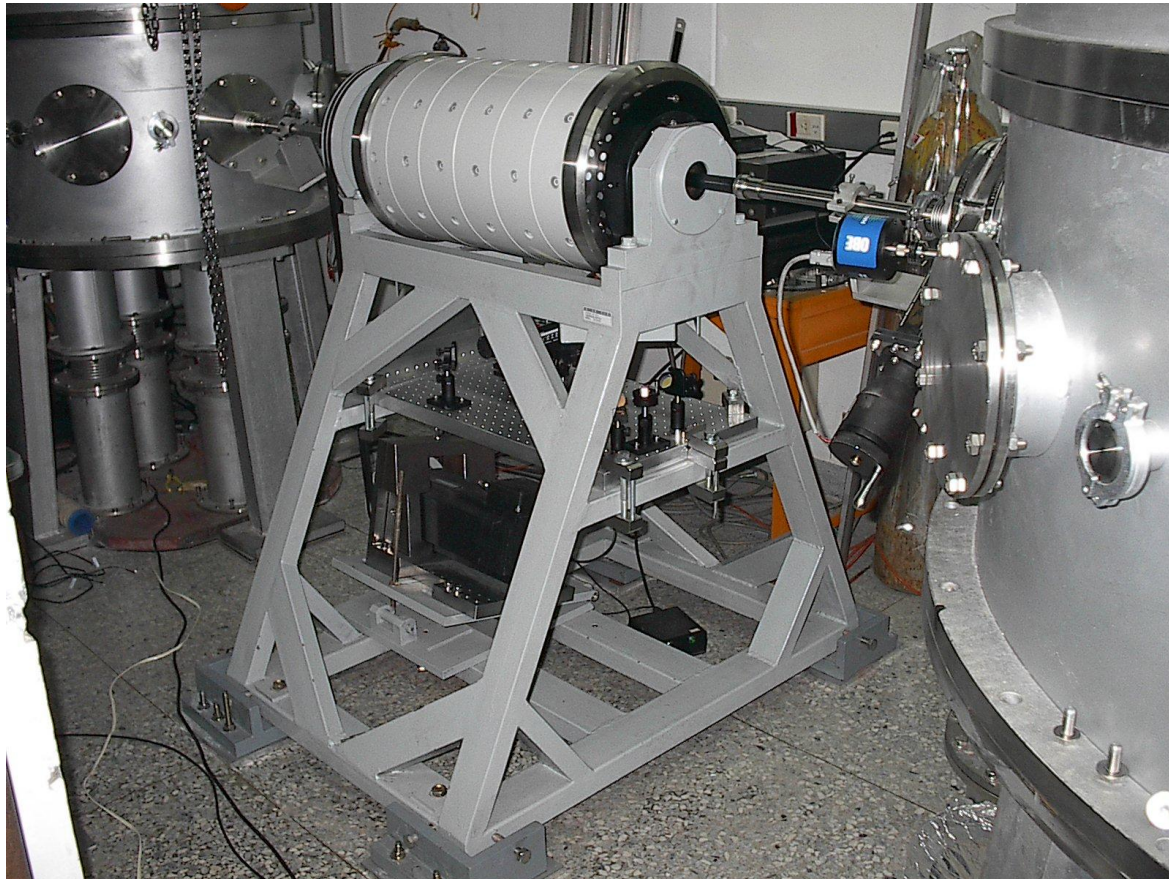


Fig. 6. Data and fitting for the measurement of the extinction ratio of No. 4 analyzer.

Injection Optical Bench



Vacuum Chamber and Magnet





Current Optical Experiments

Table 2. Current laser experiments for detecting dark matter candidates, pseudoscalar-photon interaction, or aiming at nonlinear QED effects.

Collaboration	running	results in ε	results in ψ	results in LSW	aiming at ψ_{QED}
ALPS	✓			$\sqrt{37}$	
BFRT		$\sqrt{26}$	$\sqrt{26}$	$\sqrt{26}$	
BMV	✓			$\sqrt{30,31}$	✓
GammeV	✓			$\sqrt{32,33}$	
LIPSS	✓			$\sqrt{34,35}$	
OSQAR	✓			$\sqrt{36}$	
PVLAS LNL		$\sqrt{27,28}$	$\sqrt{28}$	$\sqrt{28}$	✓
PVLAS Ferrara	✓				✓
Q & A	✓	$\sqrt{29}$			✓

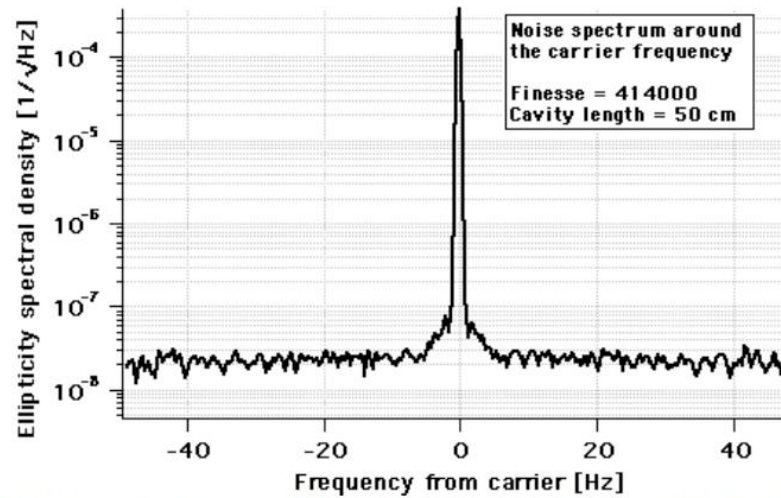
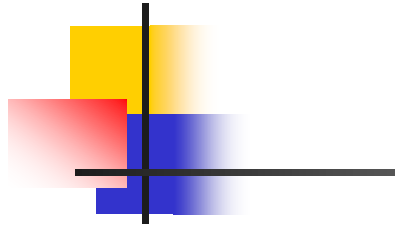


Fig. 2: Ellipticity spectral density around the modulator's carrier frequency. The ellipticity noise is flat for frequencies above about 6 Hz from the carrier.

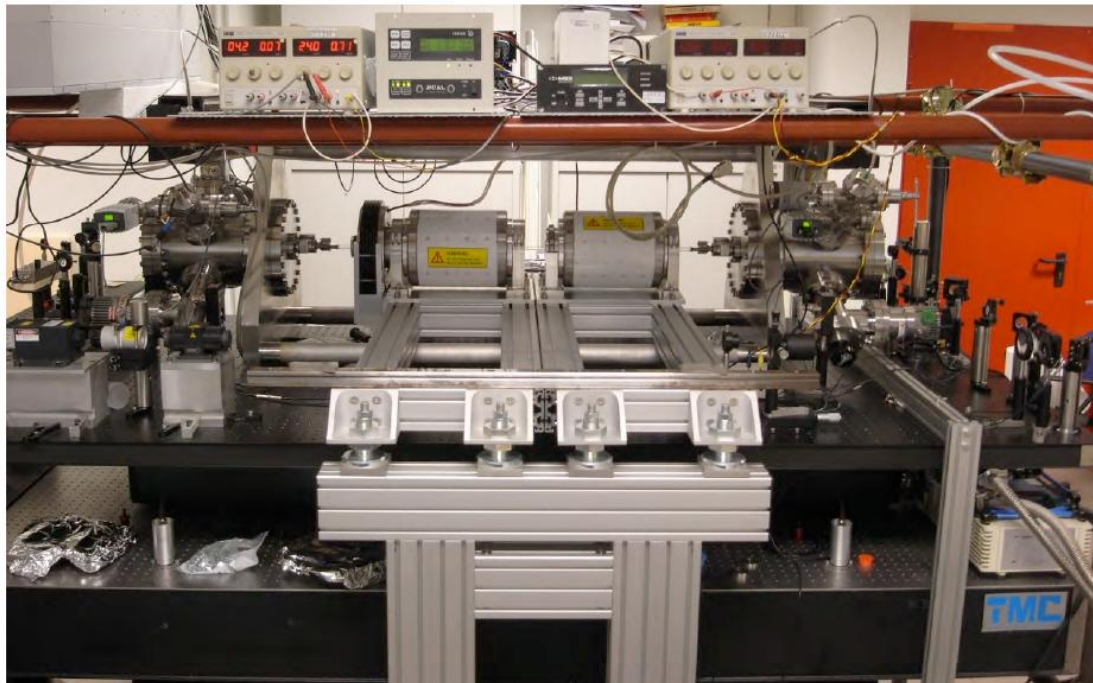


Fig. 3: Picture of the present set-up in Ferrara. The FP is 140 cm long and is supported by a two stage seismic isolation system. The Pyrex tube, 7 mm inner diameter, can be seen passing through the magnets.

Comparisons on the N2 magnetic birefringence measurement (Now: 2-3 orders away from QED detection)

Ref.	$\Delta n_{\parallel} \times 10^{-13}$ (at $P = 1\text{atm}$ and $B = 1\text{T}$)
PVLAS 2004 [30]	-2.17 ± 0.21
Q&A 2009 [31]	$-2.02 \pm 0.16 \pm 0.08$
BMV2011 This work	$-2.00 \pm 0.08 \pm 0.06$

TABLE III: Comparison between our value of the nitrogen normalized magnetic birefringence and other experimental published values at $\lambda = 1064\text{ nm}$.

- Good Calibration Consistency of the 3 Experiments

(Pseudo)scalar field: WEP & EEP with EM field

A NON-METRIC THEORY OF GRAVITY*

PHYSICAL REVIEW LETTERS

Wei-Tou Ni

Department of Physics, Montana State University

Bozeman, Montana

59715

December, 1973

VOLUME 38

14 FEBRUARY 1977

NUMBER 7

Equivalence Principles and Electromagnetism*

Wei-Tou Ni

Department of Physics, Montana State University, Bozeman, Montana 59715, and Department of Physics,
National Tsing Hua University, Hsinchu, Taiwan, Republic of China†

(Received 16 June 1976)

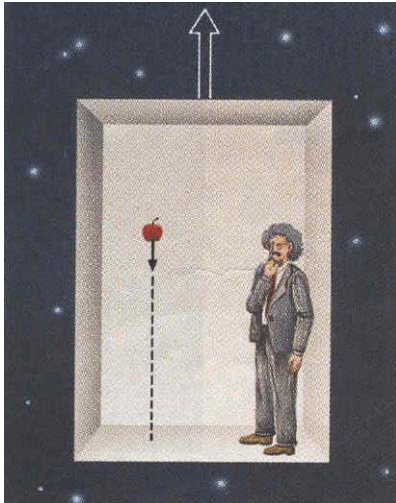
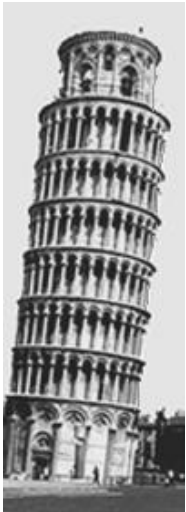
The implications of the weak equivalence principles are investigated in detail for electromagnetic systems in a general framework. In particular, I show that the universality of free-fall trajectories {Galileo weak equivalence principle (WEP(I))} does *not* imply the validity of the Einstein equivalence principle (EEP). However, WEP(II) plus the universality of free-fall rotation states (WEP(III)) *does* imply EEP. To test WEP(II) and EEP, I suggest that Eötvös-type experiments on polarized bodies be performed.

(Pseudo)scalar-Photon
Interaction



$$L_I = -(1/16\pi)\phi F_{ij}F_{kl}e^{ijkl}$$

$$F \equiv A_{j,i} - A_{i,j} \quad e^{0123} = 1$$



Modified Maxwell Equations → Polarization Rotation in EM Propagation
(Classical effect)

Constraints from CMB polarization observation → **later in this talk**

Galileo's experiment on inclined plane (Contemporary painting of Giuseppe Bezzuoli)

Galileo Equivalence Principle:
Universality of free-fall trajectories



GP-B and Rotational EP

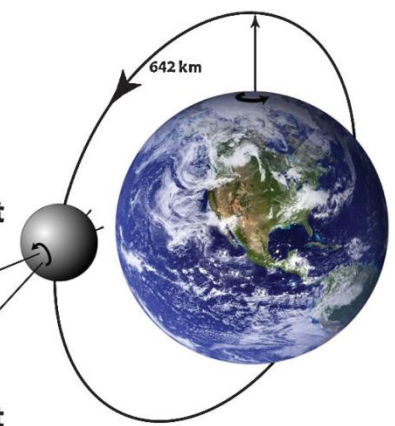
Frame-dragging Effect

-39 mas/yr WE

Guide Star
IM Pegasi
(HR 8703)

Geodetic Effect

-6606 mas/yr NS



PRL 107, 051103 (2011)

PHYSICAL REVIEW LETTERS

week ending
29 JULY 2011

Rotation, the Equivalence Principle, and the Gravity Probe B Experiment

The ultraprecise Gravity Probe B experiment measured the frame-dragging effect and geodetic precession on four quartz gyros. We use this result to test WEP II (weak equivalence principle II) which includes rotation in the universal free-fall motion. The free-fall Eötvös parameter η for a rotating body is $\leq 10^{-11}$ with a four-order improvement over previous results. The anomalous torque per unit angular momentum parameter λ is constrained to $(-0.05 \pm 3.67) \times 10^{-15} \text{ s}^{-1}$, $(0.24 \pm 0.98) \times 10^{-15} \text{ s}^{-1}$, and $(0 \pm 3.6) \times 10^{-13} \text{ s}^{-1}$, respectively, in the directions of geodetic effect, frame-dragging effect, and angular momentum axis; the dimensionless frequency-dependence parameter κ is constrained to $(1.75 \pm 4.96) \times 10^{-17}$, $(1.80 \pm 1.34) \times 10^{-17}$, and $(0 \pm 3) \times 10^{-14}$, respectively.

Lense-Thirring effect on Gyros -- Schiff Effect

- L. I. Schiff, Phys. Rev. Lett. 4, 215 (1960).
- G. E. Pugh, Research memorandum 11, Weapons System Evaluation Group, the Pentagon, Washington, DC, 1959, reprinted in Nonlinear Gravitodynamics. The Lense-Thirring Effect., edited by R. J. Ruffini and C. Sigismondi (World Scientific, Singapore, 2003), pp. 414–426.

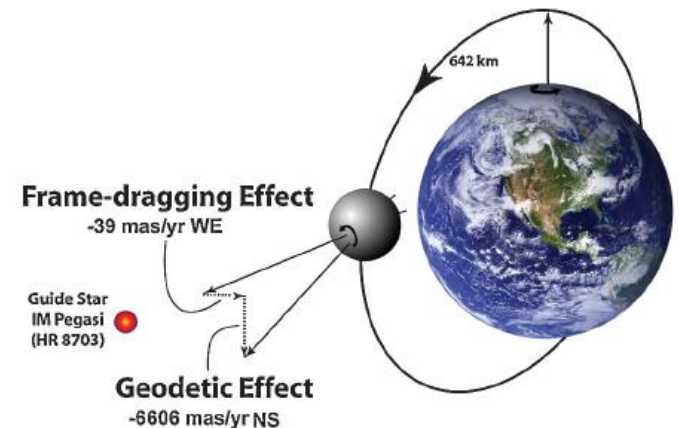


FIG. 1 (color). Predicted drift rates of GP-B gyroscopes. See [17] for definitions of WE and NS inertial directions.

$$\phi = -\frac{GM}{r}, \quad \vec{g} = -\frac{Gm}{r^2} \hat{r} \quad \vec{h} = \frac{2GI}{r^2} \vec{\omega} \times \hat{r},$$

$$\vec{\Omega} = \frac{2GI}{r^3} [3(\hat{r} \cdot \vec{\omega})\hat{r} - \vec{\omega}], \quad (2.10)$$

where $\vec{\omega}$ is the spin and I is the moment of inertia of the sphere; for a uniform density sphere $I = (3/5)Mr_s^2$ [14]. The fields in Eq. (2.10) are of course time independent.

THE LENSE-THIRRING EFFECT AND ACCRETION DISKS AROUND KERR BLACK HOLES*

JAMES M. BARDEEN AND JACOBUS A. PETTERSON

Physics Department, Yale University

Received 1974 September 10

ABSTRACT

Astrophysical evidence for the relativistic Lense-Thirring effect could come from its influence on tilted accretion disks around Kerr black holes. We show here how it causes the gradual transition of the disk into the equatorial plane of the black hole in the region between the radii 10^4M and 10^2M . We expect that a considerable part of the radiation emitted in the central part of the disk may be reabsorbed in the transition region, which may lead to observable changes in the X-ray spectrum.

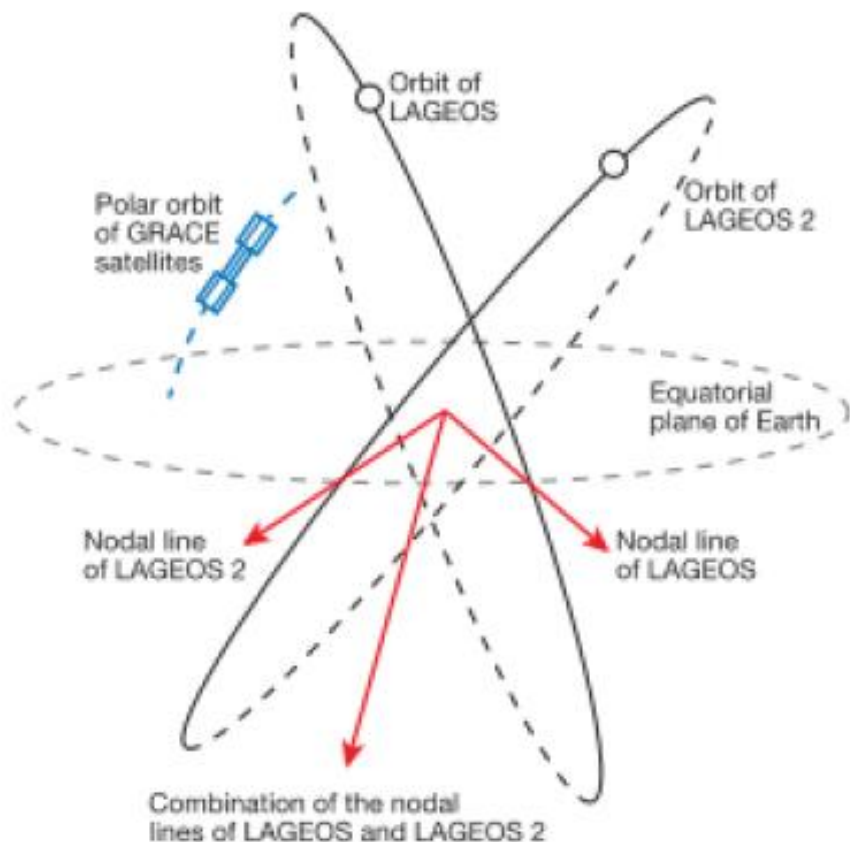
[The Astrophysical Journal, 195: L65-L67, 1975 January 15](#)

is the coupling between the spin of the black hole and the orbital angular momentum of the test particle, known in the weak-field limit as the Lense-Thirring effect. It causes a precession of the plane of a circular geodesic orbit about the rotation axis of the black hole, with angular velocity (see Wilkins 1972)

$$\omega \approx 2Jr^{-3},$$

where J is the angular momentum of the black hole. The precession due to the quadrupole moment of the black hole is less important ($\omega \sim J^2M^{-3/2}r^{-7/2}$). The Einstein perihelion precession, $\omega \sim M^{3/2}r^{-5/2}$, does not affect the orbital plane.

LAGEOS orbital gyroscope



- The 'orbital gyroscope' used to measure the Lense–Thirring effect. The 'gyroscope', indicated by the long red arrow, is the combination of the nodal longitudes of the LAGEOS satellites; it is not affected by the huge nodal rate of the LAGEOS satellites because of the Earth's quadrupole moment.
- it is independent of the residual nodal rates due to the error in the Earth quadrupole moment.
- The blue drawing shows the orbital configuration of the GRACE satellites used to accurately determine the Earth's gravity field.

LAGEOS results (GRACE launched on 17 March 2002)

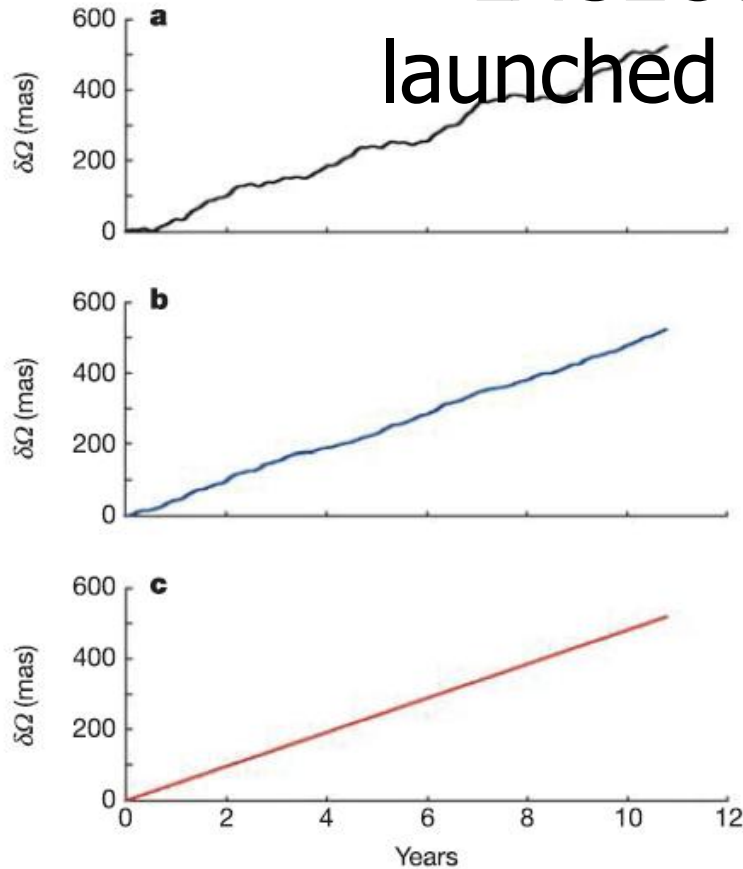


Figure 2 Observed orbital residuals of the LAGEOS satellites. The residual nodal longitudes of the LAGEOS satellites, $\delta\Omega$, were combined according to equation (1). In black (a) is the raw, observed, residual nodal longitude of the LAGEOS satellites without removal of any signal, whereas in blue (b) is the observed residual nodal longitude after removal of six periodic signals. The best-fit line (13-parameter fit) through these observed residuals has a slope of 47.9 mas yr^{-1} . In red (c) is the theoretical Lense–Thirring prediction of Einstein’s general relativity for the combination (equation (1)) of the nodal longitudes of the LAGEOS satellites; its slope is 48.2 mas yr^{-1} .

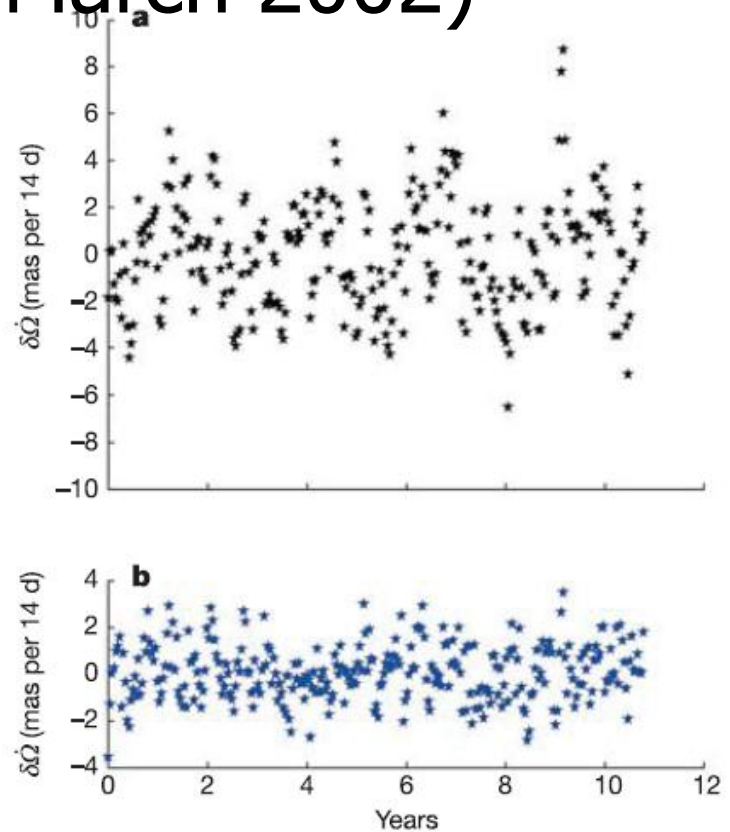


Figure 3 Post-fit orbital residuals of the LAGEOS satellites. These, 14-day, residuals of the nodal rates, $\delta\dot{\Omega}$, combined using equation (1), correspond to the case (a) of the fit of a secular trend only (black stars) and to the case (b) of a trend plus phase and amplitude of six periodic signals (blue stars) with periods of 1,044, 905, 281, 569, 111 and 284.5 days. We also fitted the residuals with a straight line plus the two LAGEOS nodal frequencies and plus ten signals. The maximum relative variation in the measured value of the Lense–Thirring effect in all the different fits was 2%.



Einstein Equivalence Principle

- EEP:(Einstein Elevator): Local physics is that of Special relativity
- Study the relationship of Galileo Equivalence Principle and EEP in a Relativistic Framework: $\chi - g$ framework --- A general phenomenological framework for studying the coupling of gravity to electromagnetism
- The photon sector of many frameworks are included:
e.g.,
SME – Standard Model Extension
SMS – Standard Model Supplement

Electromagnetism: Charged particles and photons

Special Relativity

$$L_I = -\left(\frac{1}{16\pi}\right) \eta^{ijkl} \eta^{jl} F_{ij} F_{kl} - A_k j^k (-g)^{1/2} - \sum_I m_I \frac{ds_I}{dt} \delta(x - x_I)$$

$\chi - g$ framework

$$L_I = -\left(\frac{1}{16\pi}\right) \chi^{ijkl} F_{ij} F_{kl} - A_k j^k (-g)^{1/2} - \sum_I m_I \frac{ds_I}{dt} \delta(x - x_I)$$

Galileo EP constrains χ to:

$$\chi^{ijkl} = (-g)^{1/2} \left[\frac{1}{2} g^{ik} g^{jl} - \frac{1}{2} g^{il} g^{kj} + \eta \Psi \varepsilon^{ijkl} \right]$$

(Pseudo)scalar-Photon
Interaction



Various terms in the Lagrangian

(W-T Ni, Reports on Progress in Physics, 2010 /also in arXiv)

Table 1. Various terms in the Lagrangian and their meaning.

Term	Dimension	Reference	Meaning
$e^{\alpha\beta\gamma} A_\alpha F_{\beta\gamma}$	3	Chern-Simons ³⁸ (1974)	Integrand for topological invariant
$e^{ijkl} \varphi F_{ij} F_{kl}$	4	Ni ^{22,23,24} (1973, 1974, 1977)	Pseudoscalar-photon coupling
$e^{ijkl} \varphi F_{ij}^{QCD} F_{kl}^{QCD}$	4	Peccei-Quinn ¹² (1977) Weinberg ¹³ (1978) Wilczek ¹⁴ (1978)	Pseudoscalar-gluon coupling
$e^{ijkl} V_i A_j F_{kl}$	4	Carroll-Field-Jackiw ³⁹ (1974)	External constant vector coupling

Empirical Constraints: No Birefringence

The most tested part of equivalence is the Galileo equivalence principle (the universality of free-fall). In the study of the theoretical relations between the Galileo equivalence principle and the Einstein equivalence principle, we^{33,34} proposed the $\chi - g$ framework summarized in the following interaction Lagrangian density

$$L_I = -\left(\frac{1}{16\pi}\right)\chi^{ijkl}F_{ij}F_{kl} - A_k j^k (-g)^{(1/2)} - \Sigma_I m_I (ds_I)/(dt)\delta(\mathbf{x} - \mathbf{x}_I), \quad (3)$$

The condition for no birefringence (no splitting, no retardation) for electromagnetic wave propagation in all directions in the weak field limit gives ten constraints on the χ 's. With these ten constraints, χ can be written in the following form

$$\chi^{ijkl} = (-H)^{1/2}[(1/2)H^{ik}H^{jl} - (1/2)H^{il}H^{kj}]\psi + \varphi e^{ijkl}, \quad (4)$$

where H equals $\det(H_{ij})$, H_{ij} is a metric which generates the light cone for electromagnetic propagation, and e^{ijkl} is the completely antisymmetric symbol with $e^{0123} = 1$.³⁵⁻³⁷ Recently, Lämmerzahl and Hehl have shown that this non-birefringence guarantees, without approximation, Riemannian light cone, i.e. Eq. (4).³⁸

20 W.-T. Ni, Equivalence principles and precision experiments, in *Precision Measurement and Fundamental Constants II*, National Bureau of Standards Special Publication No. 617, eds. B. N. Taylor and W. D. Phillips (U.S. Government Printing Office, Washington D.C., US, 1984), pp. 647-651.

Empirical Constraints from Unpolarized EP Experiment: constraint on Dilaton for EM:

$$\varphi = 1 \pm 10^{-10}$$

Eötvös–Dicke experiments^{9,14,41–43} are performed on unpolarized test bodies; the latest such experiments⁴³ reach a precision of 3×10^{-13} . In essence, these experiments show that unpolarized electric and magnetic energies follow the same trajectories as other forms of energy to certain accuracy. The constraints on Eq. (4) are

$$\frac{|1 - \psi|}{U} < 10^{-10} \quad (6)$$

and

$$\frac{|H_{00} - g_{00}|}{U} < 10^{-6}, \quad (7)$$

where U is the solar gravitational potential at the earth.

Cho and Kim, Hierarchy Problem, Dilatonic Fifth, and Origin of Mass, ArXiv0708.2590v1
(4+3)-dim unification with $G=SU(2)$, $L < 44 \mu\text{m}$ (Kapner et al., PRL 2007) $L < 10 \mu\text{m}$
Li, Ni, and Pulido Paton, ArXiv0708.2590v1 gr-qc Lamb shift in Hydrogen and Muonium

Empirical constraints: $H \rightarrow g$ (One Metric)

In Hughes–Drever experiments³⁹ $\Delta m/m \leq 0.5 \times 10^{-28}$ or $\Delta m/m_{\text{e.m.}} \leq 0.3 \times 10^{-24}$ where $m_{\text{e.m.}}$ is the electromagnetic binding energy. Using Eq. (4) in Eq. (3), we have three kinds of contributions to $\Delta m/m_{\text{e.m.}}$. These three kinds are of the order of (i) $(H_{\mu\nu} - g_{\mu\nu})$, (ii) $(H_{0\mu} - g_{0\mu})v$, and (iii) $(H_{00} - g_{00})v^2$ respectively.^{35,40} Here the Greek indices μ, ν denote space indices. Considering the motion of laboratories from earth rotation, in the solar system and in our galaxy, we can set limits on various components of $(H_{ij} - g_{ij})$ from Hughes–Drever experiments as follows:

$$\begin{aligned} \frac{|H_{\mu\nu} - g_{\mu\nu}|}{U} &\leq 10^{-18}, \\ \frac{|H_{0\mu} - g_{0\mu}|}{U} &\leq 10^{-13} - 10^{-14}, \\ \frac{|H_{00} - g_{00}|}{U} &\leq 10^{-10}, \end{aligned} \tag{5}$$

where $U(\sim 10^{-6})$ is the galactical gravitational potential.

Constraint on axion: $\varphi < 0.1$

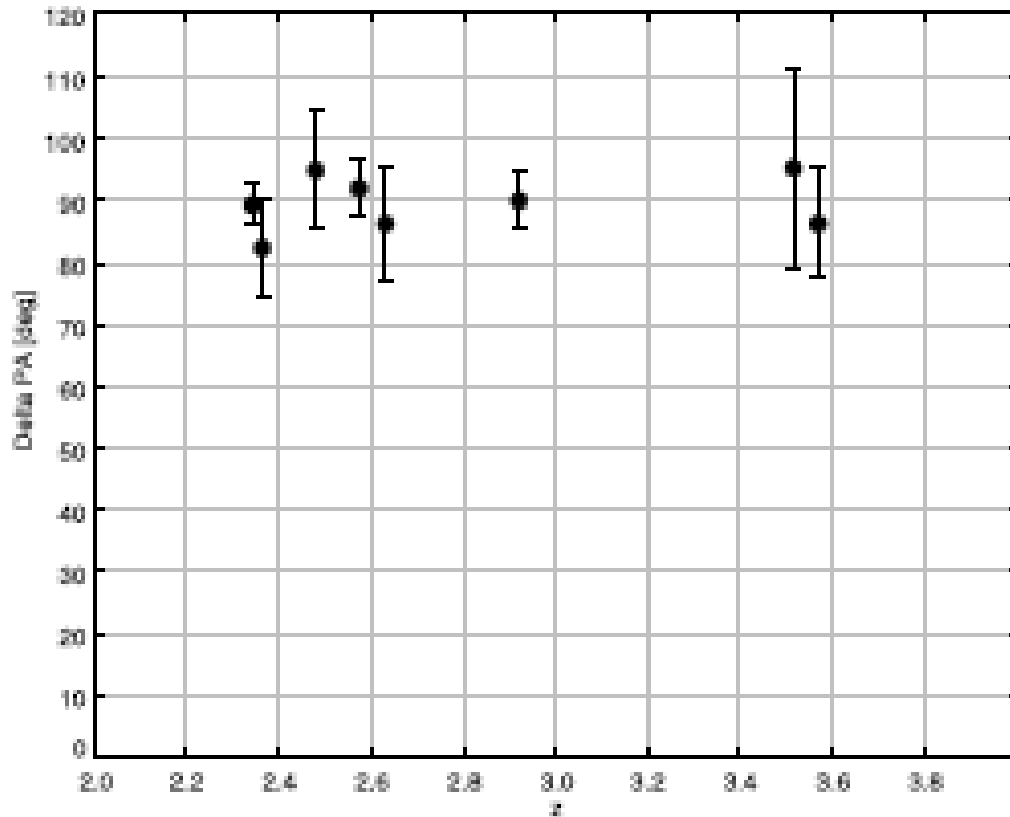
Solar-system 1973 ($\varphi < 10^{10}$)

- Metric Theories of Gravity
- General Relativity
- Einstein Equivalence Principle
recovered
- For a recent exposition of this, see Hehl & Obukhov ArXiv:0705.3422v1

Change of Polarization due to Cosmic Propagation

- The effect of φ is to change the phase of two different circular polarizations of electromagnetic-wave propagation in gravitation field and gives polarization rotation for linearly polarized light.[6-8]
- Polarization observations of radio galaxies put a limit of $\Delta\varphi \leq 1$ over cosmological distance.[9-14]
- Further observations to test and measure $\Delta\varphi$ to 10^{-6} is promising.
- The natural coupling strength φ is of order 1. However, the isotropy of our observable universe to 10^{-5} may leads to a change $(\xi)\Delta\varphi$ of φ over cosmological distance scale 10^{-5} smaller. Hence, observations to test and measure $\Delta\varphi$ to 10^{-6} are needed.

The angle between the direction of linear polarization in the UV and the direction of the UV axis for RG at $z > 2$. The angle predicted by the scattering model is 90°



- The advantage of the test using the optical/UV polarization over that using the radio one is that it is based on a physical prediction of the orientation of the polarization due to scattering, which is lacking in the radio case,
- and that it does not require a correction for the Faraday rotation, which is considerable in the radio but negligible in the optical/UV.

Limits on Cosmological Birefringence from the UV Polarization of Distant Radio Galaxies

Sperello di Serego Alighieri

INAF - Osservatorio Astrofisico di Arcetri, Largo E. Fermi 5, I-50125 Firenze - Italy

Fabio Finelli¹ and Matteo Galaverni

INAF-IASF Bologna, Via Gobetti 101, I-40129 Bologna - Italy

Table 2. Linear far UV scattering polarization in distant RG.

RG name	RA. [deg]	Dec. [deg]	z	P [%]	Pol. PA [deg]	UV PA [deg]	Δ PA [deg]	θ (1σ) [deg]
MRC 0211-122	33.5726	-11.9793	2.34	19.3 \pm 1.15 ^a	25.0 \pm 1.8	116 \pm 3 ^b	89.0 \pm 3.5	-4.5 < θ < 2.5
4C -00.54	213.3131	-0.3830	2.363	8.9 \pm 1.1 ^c	86 \pm 6	4 \pm 5 ^b	82 \pm 8	-16 < θ < 0
4C 23.56a	316.8111	23.5289	2.482	15.3 \pm 2.0 ^c	178.6 \pm 3.6	84 \pm 9 ^d	94.6 \pm 9.7	-5.1 < θ < 14.3
TXS 0828+193	127.7226	19.2210	2.572	10.1 \pm 1.0 ^a	121.6 \pm 3.4	30 \pm 3 ^b	91.6 \pm 4.5	-2.9 < θ < 6.1
MRC 2025-218	306.9974	-21.6825	2.63	8.3 \pm 2.3 ^e	93.0 \pm 8.0	7 \pm 5 ^b	86 \pm 9	-13 < θ < 5
TXS 0943-242	146.3866	-24.4804	2.923	6.6 \pm 0.9 ^a	149.7 \pm 3.9	60 \pm 2 ^b	89.7 \pm 4.4	-4.7 < θ < 4.1
TXS 0119+130	20.4280	13.3494	3.516	7.0 \pm 1.0 ^f	0 \pm 15	85 \pm 5 ^e	95 \pm 16	-11 < θ < 21
TXS 1243+036	191.4098	3.3890	3.570	11.3 \pm 3.9 ^a	38.0 \pm 8.3	132 \pm 3 ^b	86.0 \pm 8.8	-12.8 < θ < 4.8
Mean			2.80				89.2 \pm 4.2	-5.0 < θ < 3.4

Constraints on cosmic polarization rotation from CMB polarization observations

All consistent with null detection at 2σ level

[See Ni, RPP 73, 056901 (2010) for detailed references]

Analysis	Constraint [mrad]	Source data
Ni (2005a, b)	± 100	WMAP1 (Bennett <i>et al</i> 2003)
Feng, Li, Xia, Chen & Zhang (2006)	-105 ± 70	WMAP3 (Spergel <i>et al</i> 2007) & BOOMERANG (B03) (Montroy <i>et al</i> 2006)
Liu, Lee & Ng (2006)	± 24	BOOMERANG (B03) (Montroy <i>et al</i> 2006)
Kostelecky & Mews (2007)	209 ± 122	BOOMERANG (B03) (Montroy <i>et al</i> 2006)
Cabella, Natoli & Silk (2007)	-43 ± 52	WMAP3 (Spergel <i>et al</i> 2007)
Xia, Li, Wang & Zhang (2008)	-108 ± 67	WMAP3 (Spergel <i>et al</i> 2007) & BOOMERANG (B03) (Montroy <i>et al</i> 2006)
Komatsu <i>et al</i> (2009)	-30 ± 37	WMAP5 (Komatsu <i>et al</i> 2009)
Xia, Li, Zhao & Zhang (2008)	-45 ± 33	WMAP5 (Komatsu <i>et al</i> 2009) & BOOMERANG (B03) (Montroy <i>et al</i> 2006)
Kostelecky & Mews (2008)	40 ± 94	WMAP5 (Komatsu <i>et al</i> 2009)
Kahniashvili, Durrer & Maravin (2008)	± 44	WMAP5 (Komatsu <i>et al</i> 2009)
Wu <i>et al</i> (2009)	$9.6 \pm 14.3 \pm 8.7$	QuaD (Pryke <i>et al</i> 2009)
Brown <i>et al.</i> (2009)	$11.2 \pm 8.7 \pm 8.7$	QuaD (Brown <i>et al</i> 2009)
Komatsu <i>et al.</i> (2011)	$-19 \pm 22 \pm 26$	WMAP7 (Komatsu <i>et al</i> 2011)

COSMOLOGICAL MODELS to be tested



- PSEUDO-SCALAR COSMOLOGY, e.g., Brans-Dicke theory with pseudoscalar-photon coupling
- NEUTRINO NUMBER ASYMMETRY
- BARYON ASYMMETRY
- SOME other kind of CURRENT
- LORENTZ INVARIANCE VIOLATION
- CPT VIOLATION
- DARK ENERGY (PSEUDO)SCALAR COUPLING
- OTHER MODELS

Lorentz-violating vs ghost gravitons: the example of Weyl gravity (Test??)

Ghost or no Ghost or Change of Paradigm → Solar-system tests

Journal of Cosmology and Astroparticle Physics
An IOP and SISSA journal

**Helicity Decomposition of Ghost-free
Massive Gravity**

**Inflation with a Weyl term, or ghosts
at work**

Nathalie Deruelle,^a Misao Sasaki,^{b,c} Yuuiti Sendouda^{d,a} and
Ahmed Youssef^a

Claudia de Rham,^{1,2} Gregory Gabadadze³ and Andrew J. Tolley²

¹Département de Physique Théorique and Center for Astroparticle Physics, Université de Genève, 24 Quai E. Ansermet, CH-1211 Genève

²Department of Physics, Case Western Reserve University, 10900 Euclid Ave, Cleveland, OH 44106, USA

³Center for Cosmology and Particle Physics, Department of Physics, New York University, NY, 10003, USA

Lorentz-violating vs ghost gravitons: the example of Weyl gravity

Nathalie Deruelle,¹ Misao Sasaki,² Yuuiti Sendouda,^{3,1,2} and Ahmed Youssef⁴

¹*APC, CNRS-Université Paris 7, 75205 Paris CEDEX 13, France*

²*Yukawa Institute for Theoretical Physics, Kyoto University, Kyoto 606-8502, Japan*

³*Graduate School of Science and Technology, Hirosaki University, Hirosaki, Aomori 036-8561, Japan*

⁴*Institut für Mathematik und Institut für Physik,
Humboldt-Universität zu Berlin, 12489 Berlin, Germany*

(Dated: February 15, 2012)

Solar-system tests of the DSSY inflation model with a Weyl term

To study inflation with a Weyl term, Deruelle, Sasaki, Sendouda and Youssef [5] considered the action

$$S = S_{\text{Hilbert-Einstein}} + S_{\text{scalar}} + S_{\text{Weyl}} = (1/2\kappa) \int d^4x (-g)^{1/2} R - (1/2) \int d^4x (-g)^{1/2} [\partial_\mu \phi \partial^\mu \phi + 2V(\phi)] - (\gamma_W/4\kappa) \int d^4x (-g)^{1/2} C_{\mu\nu\rho\sigma} C^{\mu\nu\rho\sigma}, \quad (1.3)$$

The first term is the Hilbert-Einstein action; the second term is the scalar action; the third term is the Weyl action. In this paper, we use the units, $\kappa = 8\pi G_N$, $c = 1$ unless otherwise specified, and adopt the $(+---)$ convention for the Minkowski metric $\eta_{\alpha\beta}$.¹ γ_W is the coupling constant of the Weyl term (the last term in the action) and has dimension $(\text{length})^2$.

$$S = S_{\text{Hilbert-Einstein}} + S_{\text{matter}} + S_{\text{Weyl}}$$

Linear Approximation and Slow-Motion Weak-Field Approximation

- Linear approximation

$$h_{\mu\nu} = (-1/3)\gamma_W h^{(0W)}_{,\mu\nu} + [(4G_N)/(c^4)] \int \{ [T_{\mu\nu} - (1/2)(g_{\mu\nu}T)] / r \}_{\text{retarded}} (d^3x') + O(h^2, \gamma_W h^2).$$

- Slow-motion weak-field approximation

$$h_{\mu\nu} = -(2U/c^2)\delta_{\mu\nu} + (8/3)(\gamma_W U_{,\mu\nu}/c^2) + O(\gamma_W v^3/c^3).$$

Shapiro time delay and light deflection

$$\begin{aligned} \Delta t_S &= \int dt = (1/c) \int dz [1 + 2U - (4/3)(\gamma_W U_{,zz}) + O(h^2)] = \Delta t^N + \Delta t_S^{\text{GR}} - (4/3)(\gamma_W U_{,z})|_{z_1}^{z_2} + O(h^2) \\ &= (1/c) (z_2 - z_1) + 2(GM/c^3) \ln \{ [(z_2^2 + b^2)^{1/2} + z_2] / [(z_1^2 + b^2)^{1/2} + z_1] \} \\ &\quad + (4/3)[\gamma_W(GM/c^2)][(z_2/r_2^3) - (z_1/r_1^3)] + \gamma_W O(h^2), \quad (z_1 < 0, z_2 > 0), \end{aligned}$$

Cassini Experiment

One-way time retardation: 130 microsecond

Precision of measurement 2×10^{-5}

$$|\gamma_W| / (1 \text{ AU})^2 < 7.5 \times 10^{-4}$$

$$|\gamma_W^{1/2}| < 0.027 \text{ AU (13.5 s)}$$

Light deflection experiment less stringent

Testing DGP Scenario and Massive Gravity via Super-ASTROD

$$|d\omega/dt| = 3c/8r_c = 5 \times 10^{-4} (5 \text{ Gpc}/r_c) \text{ arcsec/century.}$$

One reason that the present constraints from the planetary motions are so relaxed is that they are nearly coplanar and for coplanar motion, universal precession cannot be detected using relative motions. Super-ASTROD has one spacecraft orbit nearly vertical to the ecliptic plane and is ideal for this measurement. Two-wavelength laser ranging through the atmosphere of Earth achieved 1 mm accuracy [1, 18]. With a single point ranging accuracy of 1 mm using pulse ranging, the DGP effect of 180 m (for a mission of 10 years: $5 \times 10^{-5} \text{ arcsec} \times 4.8 \times 10^{-6} \text{ rad/arcsec} \times 5 \text{ AU} \approx 180 \text{ m}$) for Super-ASTROD can be measured to 10^{-4} or better. For

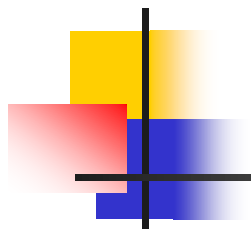
Super-ASTROD, the second-order eccentricity effect in DGP theory can also be measured. This is an example of the capability of testing relativistic gravity.



Summary and Outlook

- We look at the foundations of electromagnetism using two approaches --- to formulate a Parametrized Post-Maxwellian (PPM) framework to include QED corrections and a pseudoscalar photon interaction, and to look at gravity coupling to electromagnetism.
- We found that the foundation is solid with the only exception of a potentially possible pseudoscalar-photon interaction which can be tested using cosmological observations.
- **Precision tests of Classical Electrodynamics** will continue to serve physics community in frontier research, in the quantum regime, in gravitation and in cosmology

We have looked at possible tests of Ghosts and Massive Gravity



Thank you!